Radar Imaging with Independently Moving Transmitters and Receivers

Margaret Cheney
Department of Mathematical Sciences
Rensselaer Polytechnic Institute
Troy, NY 12180
Email: cheney@rpi.edu

Birsen Yazıcı
Electrical, Computer and Systems Engineering Department
Rensselaer Polytechnic Institute
Troy, NY 12180
Email: yazici@ecse.rpi.edu

***Abstract*— In this paper we present an analytic filtered-backpropagation inversion method for radar imaging when the transmitters and receivers are moving along independent flight paths. The flight paths are arbitrary, but assumed known. We assume a single-scattering model for the radar data, and we assume that the ground topography is known. We assume, in addition, that the receiver can correctly associate the data with the right transmitter.**

I. Introduction

For a long time there has been interest in radar imaging in the case when the transmitters and receivers are not co-located ([1], [7], [12], [13], [14], [15]). Much of this previous work deals with particularly simple trajectories such as lines and circles. In this paper we show how arbitrary trajectories can be handled.

Our approach is first to develop a physics-based model for the received signal (section II), and then to develop an approximate inversion method (section III). Our approximate inversion method is based on the microlocal-analysis techniques that were first introduced for seismic imaging ([3], [2], [5]) and were recently extended to radar imaging ([9], [10], [6], [16], [11]). These techniques give rise to filtered-backpropagation algorithms, and the resulting images have the desirable property that visible edges in the scene appear in the correct location with the correct orientation.

II. The Mathematical model

We develop the mathematical model in the frame of reference in which the target is not moving, but both transmitter and receiver may be moving.

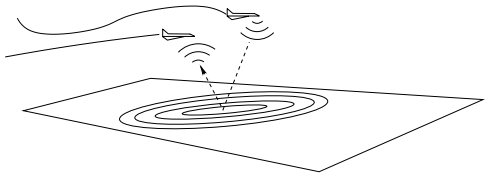

Fig. 1. Geometry

A. A model for the wave propagation

A scalar approximation to Maxwell's equations is

$$\nabla^2 E(t,\boldsymbol{x}) - (\mu_0\varepsilon(\boldsymbol{x})\ddot{E}(t,\boldsymbol{x})) = -\mu_0\dot{j}(t,\boldsymbol{x}). \quad (1)$$

where the dots denote differentiation with respect to time t, μ_0 is the magnetic permeability of free space, ε is the electric permittivity, and j is proportional to the effective current density that is the source of the field. We write $\mu_0\varepsilon(\boldsymbol{x}) = \mu_0\varepsilon_0+\rho(\boldsymbol{x}) = c_0^{-2}+\rho(\boldsymbol{x})$; this converts (1) into

$$\nabla^2 E(t,\boldsymbol{x}) - c_0^{-2}\partial_t^2 E(t,\boldsymbol{x}) = \rho(\boldsymbol{x})\ddot{E}(t,\boldsymbol{x}) - \mu_0\dot{j}(t,\boldsymbol{x}), \quad (2)$$

B. A linearized scattering model

The field incident on the reflectivity distribution ρ is the free-space field E^{in} radiating from the antenna:

$$\left(\nabla^2 - c_0^{-2}\partial_t^2\right) E^{in}(t,\boldsymbol{x}) = -\mu_0\dot{j}(t,\boldsymbol{x}) \quad (3)$$

We write $E = E^{in}+E^{sc}$ in (2) and use (3) to obtain

$$\left(\nabla^2 - c_0^{-2}\partial_t^2\right) E^{sc}(t,\boldsymbol{x}) = \rho(\boldsymbol{x})\ddot{E}(t,\boldsymbol{x}). \quad (4)$$

We can write (4) as an integral equation

$$E^{sc}(t,\boldsymbol{x}) = -\int g(t-t',\boldsymbol{x}-\boldsymbol{z})\rho(\boldsymbol{z})\ddot{E}(t',\boldsymbol{z})dt'd\boldsymbol{z}, \tag{5}$$

where the outgoing Green's function for the wave equation is

$$g(t,\boldsymbol{x}) \propto \frac{\delta(t-|\boldsymbol{x}|/c_0)}{2|\boldsymbol{x}|} = \int \frac{e^{-i\omega(t-|\boldsymbol{x}|/c_0)}}{4\pi|\boldsymbol{x}|}d\omega \tag{6}$$

A commonly used approximation [8], often called the *Born approximation* or the *single scattering approximation,* is to replace the full field E on the right side of (5) and (4) by the incident field E^{in}, which converts (5) to

$$E^{sc}_B(t,\boldsymbol{x}) \approx -\int g(t-t',\boldsymbol{x}-\boldsymbol{z})\rho(\boldsymbol{z})\ddot{E}^{in}(t',\boldsymbol{z})dt'd\boldsymbol{z} \tag{7}$$

The value of this approximation is that it removes the nonlinearity in the inverse problem: it replaces the product of two unknowns (ρ and E) by a single unknown (ρ) multiplied by the known incident field.

C. A model for the field from an antenna

The source of the field radiated from the antenna is the effective current density j on the antenna. The radiated field is the solution of (3), namely

$$E^{in}(t,\boldsymbol{x}) = \int g(t-t',\boldsymbol{x}-\boldsymbol{y})\mu_0\dot{j}(t',\boldsymbol{y})dt'\ d\boldsymbol{y}. \tag{8}$$

We note that causality is evident from (8) and (6): $E^{in}(t,\boldsymbol{x})$ is affected only by those parts of the current density $\dot{j}(t',\boldsymbol{y})$ for which $t-t' = |\boldsymbol{x}-\boldsymbol{y}|/c_0$.

We write $-\mu_0\dot{j}(t',\boldsymbol{y})$ in terms of its Fourier transform J^s:

$$\mu_0\dot{j}(t',\boldsymbol{y}) = \int e^{-i\omega t'}J^s(\omega,\boldsymbol{x})d\omega, \tag{9}$$

where ω denotes the angular frequency.

With the notation (9) and (6), (8) becomes

$$E^{in}(t,\boldsymbol{x}) = \int \frac{e^{-i\omega(t-|\boldsymbol{x}-\boldsymbol{y}|/c_0)}}{4\pi|\boldsymbol{x}-\boldsymbol{y}|}J^s(\omega,\boldsymbol{y})d\omega d\boldsymbol{y}. \tag{10}$$

Expression (10) has the advantage of showing clearly the bandlimited nature of E^{in}.

Next we assume that the antenna is small compared with the distance to the scatterers. We denote the center of the antenna by $\boldsymbol{y}^0$; thus a point on the antenna can be written $\boldsymbol{y} = \boldsymbol{y}^0 + \boldsymbol{y}'$, where $\boldsymbol{y}'$ is a vector from the center of the antenna to the point $\boldsymbol{y}$ on the antenna. In this notation, the assumption that the scattering location $\boldsymbol{x}$ is far from the antenna can be expressed $|\boldsymbol{y}'| << |\boldsymbol{x}-\boldsymbol{y}^0|$. For such $\boldsymbol{x}$, we can write

$$|\boldsymbol{x}-\boldsymbol{y}| = |\boldsymbol{x}-\boldsymbol{y}^0| - (\widehat{\boldsymbol{x}-\boldsymbol{y}^0})\cdot\boldsymbol{y}' + O(|\boldsymbol{y}'|^2/|\boldsymbol{x}-\boldsymbol{y}^0|), \tag{11}$$

where $\hat{\boldsymbol{y}}$ denotes a unit vector in the same direction as $\boldsymbol{y}$.

We use the expansion (11) in (10) to obtain

$$\begin{aligned} E^{in}(t,\boldsymbol{x},\boldsymbol{y}^0) &\approx \int \frac{e^{-i\omega(t-|\boldsymbol{x}-\boldsymbol{y}^0|/c_0)}}{4\pi|\boldsymbol{x}-\boldsymbol{y}^0|}e^{-i\omega(\widehat{\boldsymbol{x}-\boldsymbol{y}^0})\cdot\boldsymbol{y}'} \\ &\qquad J_s(\omega,\boldsymbol{y}^0+\boldsymbol{y}')d\omega d\boldsymbol{y}' \\ &\approx \int \frac{e^{-i\omega(t-|\boldsymbol{x}-\boldsymbol{y}^0|/c_0)}}{4\pi|\boldsymbol{x}-\boldsymbol{y}^0|}\hat{J}^s(\omega,\boldsymbol{x},\boldsymbol{y}^0)d\omega \end{aligned} \tag{12}$$

where we have written

$$\hat{J}^s(\omega,\boldsymbol{x},\boldsymbol{y}^0) = \int e^{-i\omega(\widehat{\boldsymbol{x}-\boldsymbol{y}^0})\cdot\boldsymbol{y}'}J^s(\omega,\boldsymbol{y}^0+\boldsymbol{y}')d\boldsymbol{y}' \tag{13}$$

This Fourier transform of the current density is the antenna beam pattern in the far field at each fixed frequency. We see from (12) that the field emanating from the antenna is a superposition of fixed-frequency point sources that are each shaped by the antenna beam pattern.

D. The received signal

The field scattered from the reflectivity distribution $\rho(\boldsymbol{z})$ due to the field (12) transmitted from position $\boldsymbol{y}$ is obtained by using (12) in (7):

$$\begin{aligned} E^{sc}_B(t,\boldsymbol{x},\boldsymbol{y}) \approx \int &\frac{e^{-i\omega(t-(|\boldsymbol{x}-\boldsymbol{z}|+|\boldsymbol{z}-\boldsymbol{y}|)/c_0)}}{(4\pi)^2|\boldsymbol{x}-\boldsymbol{z}||\boldsymbol{z}-\boldsymbol{y}|}\rho(\boldsymbol{z}) \\ &\hat{J}^s(\omega,\boldsymbol{z},\boldsymbol{y})\ \omega^2 d\omega d\boldsymbol{z} \end{aligned} \tag{14}$$

The signal received at the antenna is the convolution of the field (14) with some weight $j^r(t,\boldsymbol{y}+\boldsymbol{y}')$ that depends on the antenna characteristics and on the type of correlation reception. The receive weighting could be different from the transmit

weighting. Thus the received signal is

$$s(t) = \int E_B^{sc}(t-t', \boldsymbol{y}+\boldsymbol{y}', \boldsymbol{y}) j^r(t', \boldsymbol{y}+\boldsymbol{y}') dt' d\boldsymbol{y}' = \int \frac{e^{-i\omega(t-t'-(|(\boldsymbol{y}+\boldsymbol{y}')-\boldsymbol{z}|+|\boldsymbol{z}-\boldsymbol{y}|)/c_0)}}{(4\pi)^2 |\boldsymbol{y}+\boldsymbol{y}'-\boldsymbol{z}||\boldsymbol{z}-\boldsymbol{y}|} \rho(\boldsymbol{z}) \hat{J}^s(\omega, \boldsymbol{z}, \boldsymbol{y}) \omega^2 d\omega d\boldsymbol{z} j^r(t', \boldsymbol{y}+\boldsymbol{y}') dt' d\boldsymbol{y}' \quad (15)$$

As before, we write points on the receiving antenna as $\boldsymbol{x} = \boldsymbol{x}^0 + \boldsymbol{x}'$, make the far-field approximation and write the receiver weighting pattern j_r in terms of its temporal Fourier transform $\hat{J}^r$. Thus a model for the signal s received at position $\boldsymbol{y}$ is

$$s(t) = -\int \frac{e^{-i\omega(t-|\boldsymbol{x}-\boldsymbol{z}|/c_0-|\boldsymbol{y}-\boldsymbol{z}|/c_0)}}{(4\pi)^2 |\boldsymbol{x}-\boldsymbol{z}||\boldsymbol{z}-\boldsymbol{y}|} \rho(\boldsymbol{z}) \hat{J}^r(\omega, \boldsymbol{z}, \boldsymbol{y}) \hat{J}^s(\omega, \boldsymbol{z}, \boldsymbol{y}) \omega^2 d\omega d\boldsymbol{z} \quad (16)$$

We now assume that the transmitting antenna is moving along the path $\boldsymbol{\gamma}_j$, and the receiving antenna is moving along the path $\boldsymbol{\Gamma}_i$. Under the start-stop approximation, the data $d_{i,j}$ is

$$d_{i,j}(t,s) = \int e^{-i\omega[t-|\boldsymbol{\Gamma}_i(s)-\boldsymbol{z}|/c_0-|\boldsymbol{\gamma}_j(s)-\boldsymbol{z}|/c_0)} A_{i,j}(\omega, s, \boldsymbol{z}) d\omega \ \rho(\boldsymbol{z}) d\boldsymbol{z} \quad (17)$$

where $A_{i,j}$ is

$$A_{i,j}(\omega, s, \boldsymbol{z}) = -\frac{\hat{J}_i^r(\omega, \boldsymbol{z}, \boldsymbol{y}) \hat{J}_j^s(\omega, \boldsymbol{z}, \boldsymbol{y}) \omega^2}{(4\pi)^2 |\boldsymbol{x}-\boldsymbol{z}||\boldsymbol{z}-\boldsymbol{y}|} \quad (18)$$

We assume that each receiver can decompose the data according to which transmitter emitted the signal. This could be done by separating the transmitted signals in time, in frequency, or in their encoding.

III. Image formation

For each transmitter-receiver pair, we form the image $I_{i,j}$ by forming a weighted linear combination of the data:

$$I_{i,j}(\boldsymbol{p}) = \int e^{i\omega[t-|\boldsymbol{\Gamma}_i(s)-\boldsymbol{p}|/c_0-|\boldsymbol{\gamma}_j(s)-\boldsymbol{p}|/c_0]} B_{i,j}(\omega, s, \boldsymbol{p}) d\omega \ d_{i,j}(t,s) dt ds \quad (19)$$

where B is determined below. We note that the phase used in (19) is the negative of the phase in the model (17); this complex conjugation gives the backpropagation operation (19) a time-reversal interpretation.

The final image can be formed either coherently ($I = \sum I_{i,j}$) or noncoherently ($I = \sum |I_{i,j}|$ or $I = \sum |I_{i,j}|^2$).

Into (19) we insert (17), obtaining

$$I_{i,j}(\boldsymbol{p}) = \int K_{i,j}(\boldsymbol{p}, \boldsymbol{z}) \rho(\boldsymbol{z}) d\boldsymbol{z} \quad (20)$$

where $K_{i,j}$ is the *point spread function* or *impulse response function* or *ambiguity function*

$$K_{i,j}(\boldsymbol{p}, \boldsymbol{z}) = \int e^{-i\omega[t-|\boldsymbol{\Gamma}_i(s)-\boldsymbol{p}|/c_0-|\boldsymbol{\gamma}_j(s)-\boldsymbol{p}|/c_0]} \int e^{-i\omega'[t-|\boldsymbol{\Gamma}_i(s)-\boldsymbol{z}|/c_0-|\boldsymbol{\gamma}_j(s)-\boldsymbol{z}|/c_0)} B_{i,j}(\omega, s, \boldsymbol{p}) d\omega A_{i,j}(\omega', s, \boldsymbol{z}) d\omega' dt ds \quad (21)$$

The goal is to choose the $B_{i,j}$ so as to make $K_{i,j}$ as close to the delta function

$$\delta(\boldsymbol{p}-\boldsymbol{z}) = \frac{1}{2\pi} \int e^{i(\boldsymbol{p}-\boldsymbol{z})\cdot\boldsymbol{\xi}} d\boldsymbol{\xi} \quad (22)$$

as possible.

We simplify (21) by carrying out the t integration; this gives us

$$K_{i,j}(\boldsymbol{p}, \boldsymbol{z}) = \int e^{ik(|\boldsymbol{\Gamma}_i(s)-\boldsymbol{p}|+|\boldsymbol{\gamma}_j(s)-\boldsymbol{p}| \ e^{-ik(|\boldsymbol{\Gamma}_i(s)-\boldsymbol{z}|+|\boldsymbol{\gamma}_j(s)-\boldsymbol{z}|)} B_{i,j}(\omega, s, \boldsymbol{p}) A_{i,j}(\omega, s, \boldsymbol{z}) d\omega ds \quad (23)$$

where we have written $k = \omega/c_0$.

Next we apply the identity

$$f(\boldsymbol{p}) - f(\boldsymbol{z}) = \int_0^1 \frac{d}{d\lambda} f(\boldsymbol{z} + \lambda(\boldsymbol{p}-\boldsymbol{z})) d\lambda = (\boldsymbol{p}-\boldsymbol{z}) \cdot \int_0^1 \nabla f(\boldsymbol{y})|_{\boldsymbol{y}=\boldsymbol{z}+\lambda(\boldsymbol{p}-\boldsymbol{z})} d\lambda \quad (24)$$

to $f(\boldsymbol{z}) = |\boldsymbol{\Gamma}_i(s) - \boldsymbol{z}| - |\boldsymbol{\gamma}_j(s) - \boldsymbol{z}|$, obtaining for the phase of (23)

$$k(|\boldsymbol{\Gamma}_i(s) - \boldsymbol{p}| + |\boldsymbol{\gamma}_j(s) - \boldsymbol{p}|) - k(|\boldsymbol{\Gamma}_i(s) - \boldsymbol{z}| - |\boldsymbol{\gamma}_j(s) - \boldsymbol{z}|) = (\boldsymbol{p}-\boldsymbol{z}) \cdot \boldsymbol{\Xi}_{i,j}(\omega, s, \boldsymbol{p}, \boldsymbol{z}) \quad (25)$$

where, for $\boldsymbol{p} = \boldsymbol{z}$,

$$\boldsymbol{\Xi}_{i,j}(\omega, s, \boldsymbol{p}, \boldsymbol{p}) = k\left(\widehat{(\boldsymbol{p} - \boldsymbol{\Gamma}_i(s))} + \widehat{(\boldsymbol{p} - \boldsymbol{\gamma}_j(s))} \right) \quad (26)$$

where the hats denote unit vectors.

At this point, the vectors $\boldsymbol{p}, \boldsymbol{z}$, and $\boldsymbol{\Xi}_{i,j}$ are all three-dimensional vectors. However, the integrations in (19) and (23) are two-dimensional, which indicates that we can expect to form only a two-dimensional image. This is consistent with standard practice; typical radar images show the projection of a three-dimensional scene onto an assumed two-dimensional surface, which is generally taken to be a flat plane. Here we follow this convention: we take ρ to be of the form $\rho(\boldsymbol{z}) = \rho(\boldsymbol{z})\delta(\boldsymbol{z}_3)$, so that only the first two coordinates of $\boldsymbol{z}$ (and $\boldsymbol{p}$ and $\boldsymbol{\Xi}_{i,j}$) are relevant. To avoid complicating the notation, we continue to use simply $\boldsymbol{z}, \boldsymbol{p}$, and $\boldsymbol{\Xi}_{i,j}$; however beginning with (24) they should be considered to be two-dimensional variables.

In (23) we make the change of variables

$$(\omega, s) \to \boldsymbol{\xi}_{i,j} = \boldsymbol{\Xi}_{i,j}(\omega, s, \boldsymbol{p}, \boldsymbol{z}), \tag{27}$$

which converts (23) into

$$K_{i,j}(\boldsymbol{p}, \boldsymbol{z}) = \int e^{i(\boldsymbol{p}-\boldsymbol{z})\cdot\boldsymbol{\xi}_{i,j}} B_{i,j}(\omega, s, \boldsymbol{p}) A_{i,j}(\omega, s, \boldsymbol{z}) \left| \frac{\partial(\omega, s)}{\partial \boldsymbol{\xi}_{i,j}} \right| d\boldsymbol{\xi}_{i,j}, \tag{28}$$

where it is understood that ω and s refer to $\omega(\boldsymbol{\xi})$ and $s(\boldsymbol{\xi})$. Comparing equation (28) and (22), we see that we should choose

$$B_{i,j}(\omega, s, \boldsymbol{p}) = \frac{|\partial \boldsymbol{\xi}_{i,j}/\partial(\omega, s)|}{A_{i,j}(\omega, s, \boldsymbol{p})}, \tag{29}$$

which converts the leading order term of (28) into the desirable form

$$K_{i,j}(\boldsymbol{p}, \boldsymbol{z}) = \int_{\Omega_{\boldsymbol{p},i,j}} e^{i(\boldsymbol{p}-\boldsymbol{z})\cdot\boldsymbol{\xi}} d\boldsymbol{\xi} + (\text{smoother}) \tag{30}$$

where we have dropped the subscripts on the dummy variable and where $\Omega_{\boldsymbol{p},i,j}$ is the set of vectors swept out by (26) as ω varies over the bandwidth and s varies over values of the curve parameter for which the point $\boldsymbol{p}$ is in the antenna beams for transmitter j and receiver i. It is this set $\Omega_{\boldsymbol{p},i,j}$ that determines the resolution of the image $I_{i,j}$. In particular, from (20) and (30), we have that the leading order contribution to the image is

$$I_{i,j}(\boldsymbol{p}) = \int_{\Omega_{\boldsymbol{p},i,j}} e^{i\boldsymbol{p}\cdot\boldsymbol{\xi}} \int e^{-i\boldsymbol{z}\cdot\boldsymbol{\xi}} \rho(\boldsymbol{z}) d\boldsymbol{z} d\boldsymbol{\xi} \tag{31}$$

which shows that the reconstructed image contains precisely the Fourier components of ρ determined by the set $\Omega_{\boldsymbol{p},i,j}$.

IV. Conclusions and Future Work

We have exhibited an algorithm for producing radar images from a transmitter and receiver moving along independent and arbitrary known flight paths. These images are known ([9], [10]) to preserve visible edges in the scene.

Many interesting problems remain to be addressed. One problem is how to avoid the single-scattering approximation needed to obtain (7); one recent approach has been to use the distorted-wave Born approximation, which incorporates prior knowledge into the Green's function ([6], [11]). Another problem is how to better handle the three-dimensional nature of the scene. For example, it is possible to obtain three-dimensional scene information from multiple receivers using interferometric techniques. Another important three-dimensional issue is to include shadowing and persistence effects.

V. Acknowledgments

We are grateful to the Air Force Office of Scientific Research[1] for supporting this work under agreements FA9550-04-1-0223 and FA9550-06-1-0017.

References

[1] O. Arikan and D.C. Munson, "A tomographic formulation of bistatic synthetic aperture radar", *Proceedings of ComCon 88*, Oct. 1988, p. 418.

[2] G. Beylkin and R. Burridge, "Linearized inverse scattering problems in acoustics and elasticity", *Wave Motion* 12 (1990) 15–52.

[3] G. Beylkin, "Imaging of discontinuities in the inverse scattering problem by inversion of a causal generalized Radon transform", *J. Math. Phys.* 26 (1985) 99–108.

[4] N. Bleistein and R.A. Handelsman, *Asymptotic Expansions of Integrals*, Dover, New York, 1986.

[5] N. Bleistein, J. K. Cohen, and J.W. Stockwell, *The Mathematics of Multidimensional Seismic Inversion*, Springer, New York, 2000.

[6] M. Cheney and R.J. Bonneau, ”Imaging that exploits multipath scattering from point scatterers”, *Inverse Problems* 20 (2004) 1691-1711.
[7] A.M. Horne and G. Yates, “Bistatic synthetic aperture radar”, *IEEE Radar 2002* (Oct. 2002) 6–10.
[8] K.J. Langenberg, M. Brandfass, K. Mayer, T. Kreutter, A. Brüll, P. Felinger, D. Huo, “Principles of microwave imaging and inverse scattering”, *EARSeL Advances in Remote Sensing*, 2 (1993) 163–186.
[9] C. J. Nolan and M. Cheney, “Synthetic Aperture Inversion”, *Inverse Problems* 18 (2002) 221–236.
[10] C. J. Nolan and M. Cheney, ”Synthetic Aperture Inversion for Arbitrary Flight Paths and Non-Flat Topography”, *IEEE Trans. on Image Processing* 12 (Sept. 2003) 1035-1043.
[11] C.J. Nolan, M. Cheney, T. Dowling, and R. Gaburro, ”Enhanced angular resolutiion from multiply scattered waves”, *Inverse Problems* 22 (2006) 1817-1834.
[12] B. Rigling, *Signal processing strategies for bistatic synthetic aperture radar*, Ph.D. thesis, Ohio State University, 2003.
[13] M. Soumekh, “Bistatic synthetic aperture radar inversion with application in dynamic object imaging”, *IEEE Trans. Signal Processing* 39 (Sept. 1991) 2044–2055.
[14] M. Soumekh, “Wide-bandwidth continuous-wave monostatic/bistatic synthetic aperture radar imaging”, *Proc. Internat. Conference on Imaging Processing*3 (Oct. 1998) 361–365.
[15] N.J. Willis, *Bistatic Radar*, Artech House, Norwood, MA, 1991.
[16] B. Yazıcı, M. Cheney, and C.E. Yarman, “Synthetic-aperture inversion in the presence of noise and clutter”, *Inverse Problems* 22 (2006) 1705-1729.